John von Neumann Institute for Computing

Non-Collinear Magnetism: Exchange Parameter and T_C

Gustav Bihlmayer

published in

Computational Nanoscience: Do It Yourself!,
J. Grotendorst, S. Blügel, D. Marx (Eds.),
John von Neumann Institute for Computing, Jülich,
NIC Series, Vol. **31**, ISBN 3-00-017350-1, pp. 447-467, 2006.

http://www.fz-juelich.de/nic-series/volume31

Non-Collinear Magnetism: Exchange Parameter and T_C

Gustav Bihlmayer

Institute for Solid State Research
Forschungszentrum Jülich,
52425 Jülich, Germany
E-mail: g.bihlmayer@fz-juelich.de

The need for a reliable description of the ground state properties of complex magnetic systems as well as for the prediction of finite-temperature properties, has led to significant progress in the field of magnetic first-principles calculations. This article reviews the basic concepts of vector-spin density functional theory (DFT), *ab initio* spin dynamics, and constrained DFT. We describe the calculation of exchange parameters from a mapping of DFT results to model Hamiltonians, the determination of the magnetic ground state, and the estimation of critical temperatures from these exchange parameters. Finally, effects of spin-orbit coupling and orbital magnetism, relevant in low-dimensional magnetic systems, will be discussed.

1 Introduction

Up to now, in most *ab initio* calculations of magnetic systems only ferromagnetic – or some antiferromagnetic – states were considered. In contrast to these collinear magnetic configurations, many alloys, compounds, and even elements show non-collinear ground-states like conical or flat spin-spirals or commensurate superpositions of several spiral spin-density waves. Even in systems with collinear magnetic structures non-collinearity occurs, e.g. at domain walls or in (thermally) excited systems. To access such states from first-principles, vector-spin density functional theory (DFT) has to be applied, which treats the magnetization density as a vector field (and not as a scalar field, as in collinear DFT calculations).

From such calculations it is possible to follow several directions: like in molecular-dynamics calculations, spin-dynamics allows to study the magnetic degrees of freedom either exploring the ground state or excited state properties (like critical temperatures). Or the magnetic interactions are mapped onto a model (in the simplest case a classical Heisenberg model) and then this model is studied using parameters obtained by *ab initio* calculations. In both cases we introduce a discretization of the (vector) magnetization density: in spin-dynamics, the evolution of discrete spins, i.e. vectors attached to certain (atomic) positions, is monitored. Mapping the *ab initio* results to a model Hamiltonian which contains interactions between spins also requires that it is possible to assign a definite spin to an atom. I.e. it should be possible in the vicinity of an atom ν, e.g. within some sphere centered at the nucleus, to write the magnetization density, $\mathbf{m}(\mathbf{r})$, as

$$\mathbf{m}(\mathbf{r}) = M_\nu \hat{\mathbf{e}}_\nu \tag{1}$$

where M_ν is the magnetization and $\hat{\mathbf{e}}_\nu$ is the magnetization direction. Vector-spin DFT calculations allow to estimate whether Eq. (1) is a good approximation or not (cf. Figure 1).

In this contribution we will start with an outline of vector-spin DFT (Section 2) and the determination of stationary states (Section 2.1 and 2.2) as well as constrained DFT for

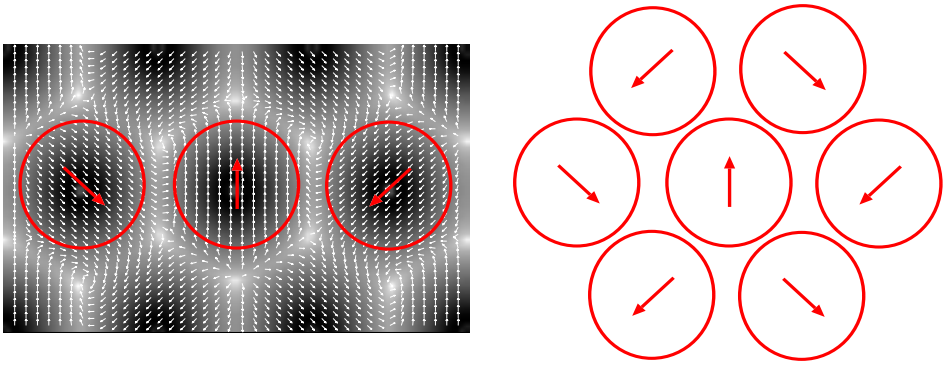

Figure 1. Left: ground state magnetization density of a hexagonal Cr monolayer with the Cu(111) in-plane lattice constant; the absolute value of the magnetization is shown in greyscale, the local directions are marked by small arrows. The average magnetization direction around an atom is indicated as red arrows. Right: schematic picture of the magnetic structure (Néel state) of the hexagonal Cr monolayer.

the calculation of non-stationary states (Section 2.3). The following sections will discuss the mapping of *ab initio* results, that have been obtained by vector-spin DFT, on models like the Heisenberg model (Section 3.1) and the determination of exchange parameters and critical temperatures (Section 3.2 and 3.3). A final chapter is then devoted to the magnetic anisotropy (Section 4) well as the relativistic effect that is mainly responsible for this anisotropy in most systems (Section 4.1). We conclude with a discussion of its influence on the ordering temperatures (Section 4.2) and the orbital magnetic moments (Section 4.3).

2 Vector-Spin Density Functional Theory

In 1964 Hohenberg and Kohn[1] worked out two central theorems that form the basis of density functional theory (DFT): For a system of N particles (e.g. electrons) moving in an external potential $v(\mathbf{r})$ (caused by e.g. nuclei) in a non-degenerate ground state (i) the many-body wavefunction Ψ and $v(\mathbf{r})$ are uniquely determined by the particle density distribution $n(\mathbf{r})$ and (ii) there exists an energy functional of this density, $E[n(\mathbf{r})]$, which is stationary with respect to variations of the ground-state density. These two theorems allow – at least in principle – the determination of the ground-state density and energy of a N-particle system. Extracting the classical Coulomb interaction energy, such a Hohenberg-Kohn energy functional takes the form

$$E[n(\mathbf{r})] = \int v(\mathbf{r})n(\mathbf{r})d\mathbf{r} + \frac{1}{2}\int\int \frac{n(\mathbf{r})n(\mathbf{r}')}{|\mathbf{r}-\mathbf{r}'|}d\mathbf{r}d\mathbf{r}' + G[n(\mathbf{r})] \tag{2}$$

where the functional $G[n(\mathbf{r})]$ has to be approximated.

In the Kohn-Sham theory[2], the kinetic energy T_0 of a non-interacting electron gas in its ground state with a density distribution $n(\mathbf{r})$ is further extracted from $G[n(\mathbf{r})]$, so that a new functional

$$E_{\mathrm{xc}}[n(\mathbf{r})] = G[n(\mathbf{r})] - T_0[n(\mathbf{r})] \tag{3}$$

remains to be determined. $E_{\rm xc}$ is now called exchange-correlation energy functional, since without $E_{\rm xc}$ our energy functional E would yield just the Hartree energy. If we take into account that particle conservation, i.e. $N = \int n(\mathbf{r}) d\mathbf{r}$ has to be ensured, we can formulate the stationarity of E in Eq. (2) with respect to variations of the ground-state density as

$$v(\mathbf{r}) + \int \frac{n(\mathbf{r}')}{|\mathbf{r} - \mathbf{r}'|} d\mathbf{r}' + \frac{\delta T_0}{\delta n(\mathbf{r})} + \frac{\delta E_{\rm xc}}{\delta n(\mathbf{r})} - \lambda = 0 \tag{4}$$

where the Lagrange parameter λ ensures the particle conservation. Expressing the kinetic energy of the non-interacting particles via their wavefunctions, ϕ_i, we can recast Eq. (4) in the form of an effective single-particle Schrödinger equation:

$$\left[-\frac{\hbar^2}{2m} \nabla^2 + v(\mathbf{r}) + \int \frac{n(\mathbf{r}')}{|\mathbf{r} - \mathbf{r}'|} d\mathbf{r}' + \frac{\delta E_{\rm xc}}{\delta n(\mathbf{r})} \right] \phi_i(\mathbf{r}) = \epsilon_i \phi_i(\mathbf{r}) \tag{5}$$

which has to be solved self-consistently since $n(\mathbf{r}) = \sum_{i=1}^{N} |\phi_i(\mathbf{r})|^2$. The last term of the Hamiltonian is called the exchange-correlation potential.

In 1972 von Barth and Hedin extended this concept to spin-polarized systems[3], replacing the scalar density by a hermitian 2×2 matrix $\underline{n}(\mathbf{r})$. If $\psi_\alpha(\mathbf{r})$ is the field operator for a particle of spin α, a component of the spin-density matrix can be defined as

$$n_{\alpha\beta}(\mathbf{r}) = \langle \Psi | \psi_\beta^+(\mathbf{r}) \psi_\alpha(\mathbf{r}) | \Psi \rangle. \tag{6}$$

The potential matrix corresponding to this spin-density matrix is denoted as $\underline{v}(\mathbf{r})$ and replaces the scalar potential. Then, we can write Eq. (5) in the form

$$\left[\left(-\frac{\hbar^2}{2m} \nabla^2 + \sum_\alpha \int \frac{n_{\alpha\alpha}(\mathbf{r}')}{|\mathbf{r} - \mathbf{r}'|} d\mathbf{r}' \right) \underline{\mathrm{I}} + \underline{v}(\mathbf{r}) + \frac{\delta E_{\rm xc}}{\delta \underline{n}(\mathbf{r})} \right] \begin{pmatrix} \phi_i^{(+)} \\ \phi_i^{(-)} \end{pmatrix} = \epsilon_i \begin{pmatrix} \phi_i^{(+)} \\ \phi_i^{(-)} \end{pmatrix} \tag{7}$$

where $\underline{\mathrm{I}}$ is a 2×2 unit matrix and the exchange-correlation potential is now also a 2×2 matrix. In terms of the Kohn-Sham wavefunctions, the density matrix can now be written as

$$n_{\alpha\beta}(\mathbf{r}) = \sum_{i=1}^{N} \phi_i^{*\alpha}(\mathbf{r}) \phi_i^{\beta}(\mathbf{r}) \quad \text{where} \quad \alpha, \beta = (+), (-). \tag{8}$$

Using the Pauli matrices, $\underline{\sigma}$, the density matrix can be decomposed into a scalar and a vectorial part, corresponding to the charge and magnetization density:

$$\underline{n}(\mathbf{r}) = \frac{1}{2} \left(n(\mathbf{r}) \underline{\mathrm{I}} + \underline{\boldsymbol{\sigma}} \cdot \mathbf{m}(\mathbf{r}) \right) = \frac{1}{2} \begin{pmatrix} n(\mathbf{r}) + m_z(\mathbf{r}) & m_x(\mathbf{r}) - i m_y(\mathbf{r}) \\ m_x(\mathbf{r}) + i m_y(\mathbf{r}) & n(\mathbf{r}) - m_z(\mathbf{r}) \end{pmatrix}. \tag{9}$$

Likewise, the potential matrices can be written in terms of a scalar potential and the magnetic field, $\mathbf{B}(\mathbf{r})$:

$$\underline{v}(\mathbf{r}) = v(\mathbf{r}) \underline{\mathrm{I}} + \mu_B \underline{\boldsymbol{\sigma}} \cdot \mathbf{B}(\mathbf{r}) \quad \text{and} \quad \underline{v}_{\rm xc}(\mathbf{r}) = v_{\rm xc}(\mathbf{r}) \underline{\mathrm{I}} + \mu_B \underline{\boldsymbol{\sigma}} \cdot \mathbf{B}_{\rm xc}(\mathbf{r}) \tag{10}$$

where $\mu_{\rm B} = \frac{e\hbar}{2mc}$ is the Bohr magneton.

2.1 Collinear and High Symmetry States

Supposing that the potential matrices in Eq. (10) are diagonal (i.e. the magnetic and exchange fields point in z direction), Eq. (7) decouples into two equations of the type of Eq. (5):

$$\left(-\frac{\hbar^2}{2m}\nabla^2 + v_{\mathrm{Coul}}(\mathbf{r}) + v(\mathbf{r}) + B_z(\mathbf{r}) + v_{\mathrm{xc}}^{(+)}(\mathbf{r})\right)\phi_i^{(+)}(\mathbf{r}) = \epsilon_i^{(+)}\phi_i^{(+)}(\mathbf{r}) \quad (11)$$
$$\left(-\frac{\hbar^2}{2m}\nabla^2 + v_{\mathrm{Coul}}(\mathbf{r}) + v(\mathbf{r}) - B_z(\mathbf{r}) + v_{\mathrm{xc}}^{(-)}(\mathbf{r})\right)\phi_i^{(-)}(\mathbf{r}) = \epsilon_i^{(-)}\phi_i^{(-)}(\mathbf{r})$$

where v_{Coul} denotes now the classical Coulomb potential and $v_{\mathrm{xc}}^{(+,-)}$ the exchange-correlation potential that arises from the functional derivative of the exchange-correlation energy with respect to the spin-up $(+)$ or spin-down $(-)$ part of the diagonal density matrix.

Systems that can be described by Eq. (11) are all kinds of magnetic materials that assume a collinear magnetic order, e.g. ferromagnetic, antiferromagnetic or ferrimagnetic states. Like the density is a property that can – at least in principle – be obtained exactly in DFT, the spin density is a property that is well defined in spin-polarized DFT:

$$\mathbf{m}(\mathbf{r}) = -\mu_{\mathrm{B}}\sum_{\alpha,\beta}\psi_\alpha^+(\mathbf{r})\boldsymbol{\sigma}_{\alpha\beta}\psi_\beta(\mathbf{r}). \quad (12)$$

The integral spin moment, M, for a collinear system is then (in units of μ_{B}) simply

$$M_{\mathrm{spin}} = \int \mathbf{m}(\mathbf{r})d\mathbf{r} = \int (n^{(+)}(\mathbf{r}) - n^{(-)}(\mathbf{r}))d\mathbf{r}. \quad (13)$$

How well this quantity corresponds to experimental values depends of course on the quality of the exchange-correlation potential that is used for an actual calculation. Some examples of results obtained in the local spin density approximation (LSDA) and generalized gradient approximation (GGA) of (spin)-moments of elemental ferromagnets are given in Table 1.

Property	source	Fe (bcc)	Co (fcc)	Ni (fcc)	Gd (hcp)
M_{spin}	LSDA	2.15	1.56	0.59	7.63
M_{spin}	GGA	2.22	1.62	0.62	7.65
M_{spin}	experiment	2.12	1.57	0.55	
$M_{\mathrm{tot.}}$	experiment	2.22	1.71	0.61	7.63

Table 1. Magnetic moments (in μ_{B} per atom) of ferromagnetic elements in the bulk. The experimentally determined total magnetization, $M_{\mathrm{tot.}}$, consists of spin- and orbital moment contributions. The LSDA results for Fe, Co and Ni are taken from Moruzzi et al.[4], the GGA values from Shallcross and coworkers[5] where also experimental values are quoted. The calculated Gd data is from Kurz et al.[6], the experimental one from White and coworkers[7].

If we come back to our original assumption, that the magnetization density in the vicinity of some atom ν should be expressible by Eq. (1), then the total energy of a magnetic system as a function of its magnetic structure can be described as a functional $E[\{\hat{\mathbf{e}}_\nu\}]$ of

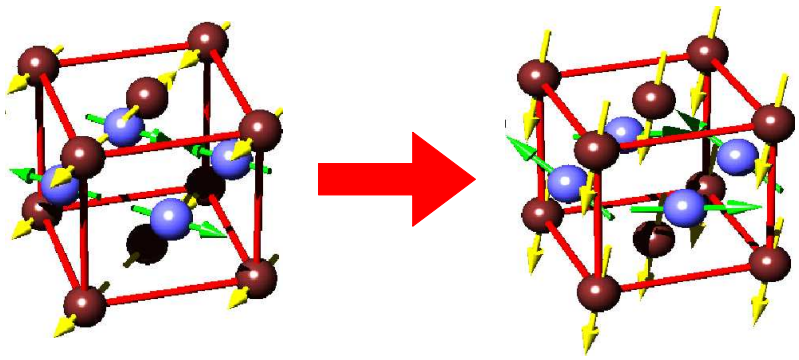

Figure 2. Determination of the magnetic ground state of ordered FeMn: the magnetic structure of the disordered alloy is a 2**q**-state (left). In an ordered alloy a more complex magnetic arrangement is obtained (right) by "relaxation" of the local spin directions.

the directions of the magnetic moments at the atoms ν in the magnetic unit cell. In this context collinear states ($\hat{\mathbf{e}}_\nu$ is identical for all atoms) are special solutions where $E[\{\hat{\mathbf{e}}_\nu\}]$ has a local or global maximum or minimum. Therefore, they constitute an important class of magnetic configurations that are often realized in magnetic materials. Unlike in non-spinpolarized DFT it is, however, in practical calculations not guaranteed that the solution obtained, $\underline{n}(\mathbf{r})$, is really the ground state, and often several metastable solutions can be obtained.

At this point we should notice, that we relied on the assumption that our functional $E[\{\hat{\mathbf{e}}_\nu\}]$ is invariant with respect to a uniform rotation of all magnetization directions, $\hat{\mathbf{e}}_\nu$. This was implicitly assumed when we arbitrarily (or, better, for convenience) selected in Eq. (11) the z direction as global magnetization axis. Indeed, in absence of an external field (or in its presence, as long as it is oriented in z direction) this implies no loss in generality, if v_{xc} is isotropic in space. If we start from a Schrödinger-Pauli like theory, there is indeed no term that could couple the spin-space to the lattice. Only if a spin-orbit coupling term (from a Dirac type theory) or – in some cases – dipolar interaction is included, a preferential direction for the collinear magnetization exists. This will be discussed in Section 4.

2.2 Spin-Dynamics, Magnetic Torque

If one is interested in the magnetic ground state of a system of given chemical composition and atomic positions, the final goal is to minimize the functional $E[\{\hat{\mathbf{e}}_\nu\}]$. The dimensionality of this problem will of course depend on the size of the unit cell chosen (some multiple of the chemical unit cell) and this minimization will involve the tricky task of determining the absolute minimum on a high-dimensional total energy surface. In analogy to molecular dynamics, i.e. the problem of minimizing the energy as a function of the atomic positions, we introduce here a spin dynamics, where the magnetic orientations, $\hat{\mathbf{e}}_\nu$, take the role of the variables.

Any vector-spin DFT calculation has to start with a reasonably chosen spin configuration in a prescribed unit cell. On a simple level, one can "relax" the directions of the magnetization at the atoms in the same way a relaxation of the atomic structure (e.g. at a

surface) is done. The magnetization directions, $\hat{\mathbf{e}}_\nu$, will then normally change to reduce the total energy (cf. Figure 2). The final magnetic state, that will be reached, will in general depend on the starting point of the calculation and a more elaborate technique will be needed to avoid being trapped in some local minimum of $E[\{\hat{\mathbf{e}}_\nu\}]$.

To this end we have to develop an equation of motion for the magnetization of an atom. To keep things simple, we will focus on the case, where the magnetization stays collinear within the vicinity of the atom. Let us start from the Hamiltonian of Eq. (7) and assume that the external potential matrix, $\underline{v}(\mathbf{r})$, has been chosen to be diagonal, and the exchange-correlation potential is separated into diagonal and off-diagonal parts. Following Antropov et al.[8,9] we use

$$\frac{\delta E_{\rm xc}}{\delta \underline{n}(\mathbf{r})} = v_{\rm xc}\underline{\rm I} - \underline{\boldsymbol{\sigma}} \cdot \mathbf{B}_{\rm xc} \quad \text{and} \quad \Phi = \begin{pmatrix} \phi^{(+)} \\ \phi^{(-)} \end{pmatrix},$$

and set up a time-dependent analogon of Eq. (7):

$$i\frac{d\Phi}{dt} = \left[H_d - \underline{\boldsymbol{\sigma}} \cdot \mathbf{B}(\mathbf{r},t)\right]\Phi, \tag{14}$$

where H_d is the Hamiltonian that contains now only diagonal parts.

We will now separate the evolution of the magnetization into fast (value of the magnetization) and slow (direction of the magnetization) degrees of freedom. The former part will be described quantum-mechanically, while the latter is treated on a semiclassical level. Let us assume a field of spin-rotation matrices, $\underline{U}(\mathbf{r},t)$, that transforms our spin coordinate system such, that the local z-axis is always in the direction of the $\mathbf{B}$-field. Using transformed basis functions, $\chi = \underline{U}\Phi$, we can reformulate Eq. (14) as

$$i\frac{d}{dt}\chi(\mathbf{r},t) = \left[H_d - \sum_\nu \underline{\sigma}_{z,\nu} B_{z,\nu}(\mathbf{r},t)\right]\chi(\mathbf{r},t). \tag{15}$$

where $B_{z,\nu}(\mathbf{r},t)$ is $\mathbf{B}(\mathbf{r},t)$ at an atom ν in a locally diagonal form. At a given time, t, the time-independent version of this equation can be solved, provided that $\underline{U}(\mathbf{r},t)$ is known. Since $\underline{U}$ follows the magnetization, we have to determine now an equation of motion for the magnetization.

The equation of motion of the magnetization, $\mathbf{m}(\mathbf{r},t)$, can be obtained by multiplying Eq. (14) from the left with $\Phi^*\underline{\boldsymbol{\sigma}}$ and adding the complex conjugate equation. Comparing this to the time derivative of Eq. (12) and using the relation $\underline{\boldsymbol{\sigma}}(\underline{\boldsymbol{\sigma}} \cdot \mathbf{B}) = \mathbf{B} - i\underline{\boldsymbol{\sigma}} \times \mathbf{B}$ we get

$$\frac{d\mathbf{m}(\mathbf{r},t)}{dt} = 2\mathbf{m} \times \mathbf{B} + \frac{i}{2}\nabla(\Phi^*\underline{\boldsymbol{\sigma}} \cdot \nabla\Phi - c.c.). \tag{16}$$

The second term on the right side is complicated and describes longitudinal changes of the magnetization, which we will not consider on this level. Omitting this term, Eq. (16) describes the precession of the magnetization direction at an atom under the influence of the magnetic field generated by the atom itself and other atoms of the crystal.

Returning once more to Eq. (1), we can simplify Eq. (16) and write the evolution of the magnetization direction in atom ν as

$$\frac{d\hat{\mathbf{e}}_\nu}{dt} = -\frac{2}{\mu_{\rm B}}\hat{\mathbf{e}}_\nu \times \mathbf{I}_\nu \tag{17}$$

where $\mathbf{I}_\nu = \mu_\mathrm{B}\mathbf{B}$. If we explicitly also want to take into account the effect of other fields acting onto a magnetization direction, e.g. stemming from the spin-orbit interaction (magnetic anisotropy) or dipole-dipole interaction, these fields can be added to $\mathbf{I}_\nu$ in Eq. (17): $\mathbf{I}_\nu \to \mathbf{I}_\nu + \mathbf{I}_\mathrm{SO} + \mathbf{I}_\mathrm{d-d}$. More general expressions of Eq. (17), suitable for spin-dynamics with finite temperatures included, can be found in Ref. 9.

The next question, that has to be answered, is how to determine the fields $\mathbf{I}_\nu$, given i.e. a certain set of magnetization directions $\{\hat{\mathbf{e}}_\nu\}$ that gives the torque on a selected magnetic moment[10]. This problem can be solved in constrained vector-spin density functional theory, as introduced in the next section.

2.3 Non-Stationary States: Constrained (VS)DFT

In general, an arbitrary magnetic configuration given by a set of local (atomic) magnetization directions $\{\hat{\mathbf{e}}_\nu\}$ is not an extremum or a stationary solution of the total energy functional $E\,[\underline{n}(\mathbf{r})]$. Exceptions are high symmetry states, like collinear magnetic states, a certain class of spin-spiral states (see Section 3.2) and particular linear superpositions of several spin-spiral states. The constrained density functional theory developed by Dederichs *et al.*[11] provides the necessary generalization to deal with arbitrary magnetic configurations, i.e. configurations where the orientations of the local moments are constrained to non-equilibrium directions. We define a generalized energy functional $\tilde{E}\,[\underline{n}(\mathbf{r})|\{\hat{\mathbf{e}}_\nu\}]$, where we ensure that the average magnetization in an atom, $\langle\mathbf{m}\rangle_\nu$, points in the direction $\hat{\mathbf{e}}_\nu$. This condition, $\hat{\mathbf{e}}_\nu \times \langle\mathbf{m}\rangle_\nu = 0$, is introduced by an Lagrange multiplier, $\boldsymbol{\lambda}$, such that[12]

$$\begin{aligned}\tilde{E}\,[\underline{n}(\mathbf{r})|\{\hat{\mathbf{e}}_\nu\}] &= E\,[\underline{n}(\mathbf{r})] + \sum_\nu \boldsymbol{\lambda}^\nu \cdot (\hat{\mathbf{e}}_\nu \times \langle\mathbf{m}\rangle_\nu) \\ &= E\,[\underline{n}(\mathbf{r})] + \mu_B \sum_\nu \mathbf{B}_c^\nu \cdot \langle\mathbf{m}\rangle_\nu. \end{aligned} \tag{18}$$

Here, we recast the Lagrange multiplier in the form of a magnetic field, $\mathbf{B}_c^\nu$. This is the constraining field in the atom ν that fixes the local (integrated) magnetic moment $\mathbf{M}^\nu$ parallel to the prescribed direction $\hat{\mathbf{e}}_\nu$. $\mathbf{M}^\nu$ is the magnetization density

$$\langle\mathbf{m}(\mathbf{r})\rangle_\nu = \mathbf{M}^\nu = \int_{MT^\nu} \mathbf{m}(\mathbf{r})\, d^3r \tag{19}$$

averaged over the sphere where Eq. (1) holds. Thus $\mathbf{B}_c^\nu$ ensures that the local moments have no components $\mathbf{M}_\perp^\nu$ normal to the directions $\hat{\mathbf{e}}_\nu$, $\hat{\mathbf{e}}_\perp^\nu$, for any atom.

The effective B-field, $\mathbf{B}_\mathrm{eff}^\nu$, that enters the muffin-tin part of the Hamiltonian is given by (here, absence of external fields is assumed for simplicity)

$$\mathbf{B}_\mathrm{eff}^\nu(\mathbf{r}) = B_\mathrm{xc}^\nu\,[\underline{n}(\mathbf{r})]\;\hat{\mathbf{e}}_\nu \;+\; B_c^\nu\,\hat{\mathbf{e}}_\perp^\nu = B_\mathrm{eff}^\nu(\mathbf{r})\,\hat{\mathbf{e}}_B^\nu(\mathbf{r}). \tag{20}$$

Even if $\mathbf{B}_\mathrm{xc}^\nu$ is assumed to be collinear in the vicinity of the atom ν (pointing in the direction $\hat{\mathbf{e}}_\nu$), the effective $\mathbf{B}$-field is again a continuous non-collinear vector field in the muffin-tin spheres, with pointwise local directions $\hat{\mathbf{e}}_B^\nu(\mathbf{r})$.

In an actual constrained local moment (CLM) calculation, $\underline{n}(\mathbf{r})$ and $\mathbf{B}_c^\nu$ have to be determined self-consistently. The density matrix is calculated in the usual self-consistency cycle. At the same time, the local constraint fields $\mathbf{B}_c^\nu$ have to be adjusted, until the constraint conditions, $\hat{\mathbf{e}}_\nu \times \langle\mathbf{m}\rangle_\nu = 0$, are fulfilled (cf. Figure 3). At the end of such a

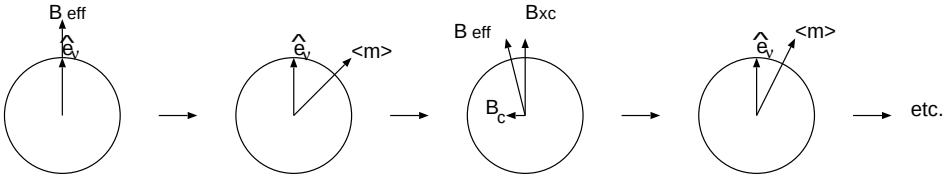

Figure 3. Determination of the constraint field: Initially, the effective $\mathbf{B}$-field is parallel to the prescribed direction $\hat{\mathbf{e}}^\nu$ (left). The resulting magnetization, $\langle \mathbf{m} \rangle$, generally is not parallel to this direction. Therefore, a constraint field $\mathbf{B}_c$ is introduced, that points in opposite direction to the component of the magnetization that is perpendicular to $\hat{\mathbf{e}}^\nu$. Using this $\mathbf{B}_{\mathrm{eff}}$, the direction of the magnetization is then adjusted towards $\hat{\mathbf{e}}^\nu$ (right).

calculation we obtain the self-consistent densities and a set of local constraint $\mathbf{B}$-fields. The total energy of the system is given by the constrained energy functional, Eq. (18).

According to the the Hellmann-Feynman theorem we find that the change of the energy due to a change in magnetization direction, $d\hat{\mathbf{e}}_\nu$, is given by $dE = -\mu_B \mathbf{M}^\nu \cdot (\mathbf{B}_c^\nu \times d\hat{\mathbf{e}}_\nu)$. Therefore, the constraint field can be interpreted as a torque acting on the magnetic moment, in the spirit of the spin dynamics, formulated in the previous section. Thus, we have set up a formalism that allows us to find – at least in principle – the magnetic ground state of a system by spin-dynamics[13]. But CLM calculations can also be used in a different way: In the next section we will describe how they can be used to determine the exchange interactions in a system and utilize these results in models, like the classical Heisenberg model, to obtain information about the ground state, but also about excited states of a magnetic system.

3 Magnetism and Exchange Interactions

Using the methods and results described in the last sections, it is possible to simulate magnetic systems and determine their ground state quite accurately. Nevertheless, such a strategy might be not very satisfactory, since spin-dynamics simulations are computationally quite demanding, may depend on computational parameters like the unit-cell size, and finally do not offer very much insight into the underlying physics that leads to the magnetic ground state. Therefore, it is sometimes useful to map the results of DFT on a physical model that can help in the interpretation of the results (Section 3.1) and suggest possible magnetic ground state structures (Section 3.2). In some cases, it is even possible to obtain non-groundstate properties from these models (Section 3.3).

3.1 The Heisenberg Model and Its Extensions

Consider a system of N electrons localized on N lattice sites, such that every lattice site is occupied by exactly one electron. Each electron is localized in an orbital $f_n(\mathbf{r}, \sigma)$ with a spin index σ. The Hamiltonian of the system will consist of a kinetic energy part, the Coulomb repulsion, and some (scalar) potential, that keeps the electrons localized. If we are only interested in energy changes that come from a change of the spin-part of the wavefunctions (i.e. the magnetic structure of the lattice), the contributions of the kinetic energy and the scalar potential can be ignored. But the Coulomb interaction, together

with the Pauli exclusion principle, can differentiate between spin structures: suppose the Coulomb energy is given by

$$V = \frac{e^2}{2} \sum_{\sigma\sigma'} \int d\mathbf{r} d\mathbf{r}' \frac{\psi^*(\mathbf{r}', \sigma')\psi^*(\mathbf{r}, \sigma)\psi(\mathbf{r}, \sigma)\psi(\mathbf{r}', \sigma')}{\mathbf{r} - \mathbf{r}'} \quad ; \quad \psi^*(\mathbf{r}, \sigma) = \sum_n c^*_{n\sigma} f^*_n(\mathbf{r}) \tag{21}$$

where $c^*_{n\sigma}$ is the creation operator of an electron of spin σ at site n. Then, generally,

$$V = \frac{e^2}{2} \sum_{\sigma\sigma'} \sum_{n_1 n_2 n_3 n_4} c^*_{n_1\sigma'} c^*_{n_2\sigma} c_{n_3\sigma} c_{n_4\sigma'} \int d\mathbf{r} \int d\mathbf{r}' \frac{f^*_{n_1}(\mathbf{r}') f^*_{n_2}(\mathbf{r}) f_{n_3}(\mathbf{r}) f_{n_4}(\mathbf{r}')}{\mathbf{r} - \mathbf{r}'}. \tag{22}$$

A single term of this sum describes the interaction of an electron with spin σ at site 3 with an electron with spin σ' at site 4, so that finally a state with electrons with spins σ' and σ at sites 1 and 2 is reached. Since all electrons are localized, we have $(n_1, n_2) = (n_3, n_4)$. Introducing the number operators $n_{n\sigma} = c^*_{n\sigma} c_{n\sigma}$, we can write:

$$\begin{aligned} V &= \frac{1}{2} \sum_{\sigma\sigma'} \sum_{nn'} (n_{n'\sigma'} n_{n\sigma} K_{nn'} + c^*_{n'\sigma'} c^*_{n\sigma} c_{n'\sigma} c_{n\sigma'} J_{nn'}) \\ K_{nn'} &= e^2 \int d\mathbf{r} \int d\mathbf{r}' |f_n(\mathbf{r})|^2 (\mathbf{r} - \mathbf{r}')^{-1} |f_{n'}(\mathbf{r}')|^2 \\ J_{nn'} &= e^2 \int d\mathbf{r} \int d\mathbf{r}' f^*_{n'}(\mathbf{r}') f^*_n(\mathbf{r}) (\mathbf{r} - \mathbf{r}')^{-1} f_{n'}(\mathbf{r}) f_n(\mathbf{r}'). \end{aligned} \tag{23}$$

The first term of Eq. (23) does not depend on the spin and can again be ignored. The second term, however, describes an exchange of spins between sites n and n' and $J_{nn'}$ is, therefore, called exchange coupling constant. Carrying out the spin summation in Eq. (23) this term becomes[14]:

$$V = -\sum_{nn'} J_{nn'} (\frac{1}{4} + \mathbf{s}_n \cdot \mathbf{s}_{n'}). \tag{24}$$

This term describes an attractive potential for electrons of the same spin at neighboring sites. It corrects the ordinary Coulomb repulsion described by K for the fact, that electrons of the same spin have to avoid each other due to the requirements of the Pauli principle.

In this picture, clearly ferromagnetism is favored. But modifications of the original assumptions (e.g. if the interaction between the sites is "mediated" by other orbitals), can also lead to antiferromagnetic couplings. In any case the Heisenberg Hamiltonian of the form

$$H = -\sum_{nn'} J_{nn'} \mathbf{s}_n \cdot \mathbf{s}_{n'} \tag{25}$$

can be used as a phenomenological starting point in the investigation of the magnetic interaction in a crystal. Although the Heisenberg model was introduced for magnetic insulators with localized moments, we can also apply Eq. (25) to metallic systems, as shown in Figure 4. In these hexagonal unsupported monolayers the behavior of the total energy as a function of the relative angle between the atoms can be described as cosine-like function, the exchange coupling constant being negative for Cr and Mn (preferring antiferromagnetic coupling) and positive for Fe (leading to a ferromagnetic ground state). The total

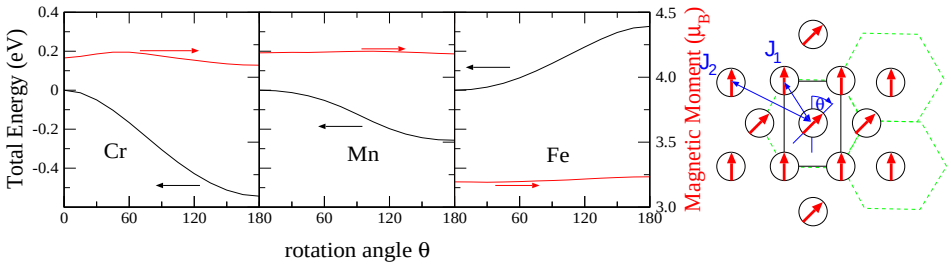

Figure 4. Total energy and magnetic moment of hexagonal monolayers of Cr, Mn, and Fe as a function of the angle of the magnetization in a two-atomic unit cell (right). $\theta = 0°$ corresponds to a ferromagnetic state, $\theta = 180°$ is a row-wise antiferromagnetic state. As lattice constant we chose the parameters of the Ag(111) surface. In the schematic picture of the hexagonal monolayer (right) the coupling to nearest neighbors (J_1) and next- nearest neighbors (J_2) is indicated.

energy has been calculated by a constrained DFT calculation as described above. We further see, that the magnetic moment does not change significantly as the spins are rotated, an important requirement for the application of the Heisenberg model.

From the right part of Figure 4 we can see, that rotating the local magnetic moment direction of one atom in the two-atom unit cell of the hexagonal lattice will change the relative orientation of that atom to four nearest neighbors, but does not affect two of the nearest neighbor (NN) atoms. Likewise, only four of the six second-NN atoms will change the relative orientation to the original atom. This leads to an expression for the total energy in the classical Heisenberg model up to second-NN:

$$E = -S^2(J_1 + J_2)(2 + 4\cos\theta) \tag{26}$$

if $\mathbf{S}$ is now the total spin moment treated as a classical vector. This means, from a constrained local moment calculation we can at least estimate the size of $(J_1 + J_2)$. It is not difficult to find other unit cells and rotations that allow the determination of other linear combinations of J_1 and J_2, thereby separating the individual exchange coupling constants[15].

Of course, the energies obtained from the CLM calculation contain contributions of all J_n and also from interactions that are not described by the Heisenberg model. Such terms can be classified with respect to an expansion of H in powers of $\mathbf{S}$, such that the Heisenberg model contains the terms up to second order (since, as discussed above, it is derived from a model taking into account pairwise interactions). The next highest terms (in absence of spin-orbit coupling effects) are then to fourth order in $\mathbf{S}$:

$$H_{\mathrm{bi-qu.}} = -\sum_{ij} B_{ij}(\mathbf{S}_i \cdot \mathbf{S}_j)^2 \quad \text{and} \tag{27}$$

$$H_{4-\mathrm{spin}} = -\sum_{ijkl} K_{ijkl}\left[(\mathbf{S}_i\mathbf{S}_j)(\mathbf{S}_k\mathbf{S}_l) + (\mathbf{S}_j\mathbf{S}_k)(\mathbf{S}_l\mathbf{S}_i) - (\mathbf{S}_i\mathbf{S}_k)(\mathbf{S}_j\mathbf{S}_l)\right].$$

The first term, the biquadratic interaction, comes from hopping processes between sites 1 and 2 like $1 \to 2 \to 1 \to 2 \to 1$, the second term, the 4-spin interaction from a hopping $1 \to 2 \to 3 \to 4 \to 1$. Terms of third order can only occur in the presence of spin-orbit

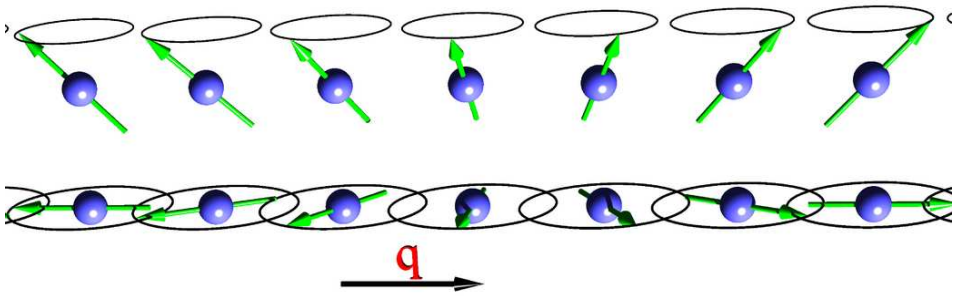

Figure 5. Spiral spin density wave (SSDW) or spin spiral propagating along a row of atoms with a wavevector $\mathbf{q}$. The opening angle is $45°$ in the upper and $90°$ in the lower example.

interaction. E.g. the so-called Dzyaloshinsky-Moriya interaction has the form:

$$H_{\mathrm{DM}} = \mathbf{D} \cdot (\mathbf{S}_1 \times \mathbf{S}_2) \tag{28}$$

and comes from anisotropic exchange interaction[16]. All these different interaction terms can be extracted from a set of suitable *ab initio* calculations (possibly including spin-orbit interaction) and used to determine the magnetic ground state within the chosen model.

3.2 Spin Spirals and the Generalized Bloch Theorem

In a periodic crystal it is convenient to replace the quantities in Eq. (25) by their Fourier-transformed equivalents:

$$\mathbf{S}(\mathbf{q}) = \frac{1}{N} \sum_n \mathbf{S}_n e^{-i\mathbf{q}\mathbf{R}_n} \quad \text{and} \quad J(\mathbf{q}) = \sum_n J_{0n} e^{-i\mathbf{q}\mathbf{R}_n}. \tag{29}$$

Exploiting the translational invariance of the lattice, we can then rewrite Eq. (25) as

$$H = -N \sum_{\mathbf{q}} J(\mathbf{q}) \mathbf{S}(\mathbf{q}) \cdot \mathbf{S}(-\mathbf{q}) \tag{30}$$

where we have to ensure that the length of all spins $\mathbf{S}_n^2 = S^2$ is conserved on all sites n. This condition is fulfilled by solutions of the type[16]

$$\mathbf{S}_n = \sqrt{2} S \left(\hat{\mathbf{e}}_x \cos(\mathbf{q} \cdot \mathbf{R}_n) + \hat{\mathbf{e}}_y \sin(\mathbf{q} \cdot \mathbf{R}_n) \right) \tag{31}$$

where the unit vectors $\hat{\mathbf{e}}_x$ and $\hat{\mathbf{e}}_y$ just have to be perpendicular to each other, otherwise their directions are arbitrary. Eq. (31) describes a spiral spin density wave (SSDW) as shown in the lower half of Figure 5. These SSDWs are general solutions of the Heisenberg model. From Eq. (30) one can conclude that the SSDW with the lowest total energy will be the one with the propagation vector $\mathbf{Q}$ which maximizes $J(\mathbf{q})$. E.g. if $\mathbf{Q} = 0$ maximizes $J(\mathbf{q})$, the solution corresponds to the ferromagnetic state, if $\mathbf{Q} = \hat{\mathbf{e}}_z \frac{\pi}{a_z}$ and a_z is the lattice constant in z-direction, then the structure is layered antiferromagnetic in z-direction. Some other examples – for a hexagonal monolayer – are illustrated in Figure 6.

SSDWs can be described by the propagation vector of the spin-spiral $\mathbf{q}$, the rotation axis (which is, when no coupling between spin and lattice is present, not fixed with respect

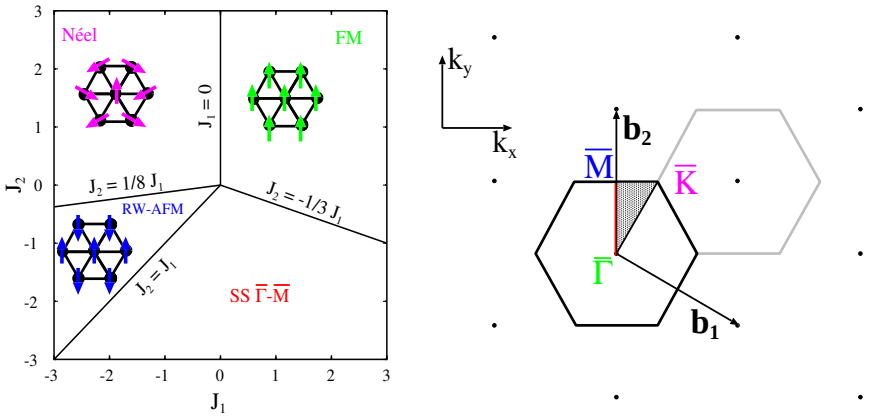

Figure 6. Phase diagram of the hexagonal lattice in next-nearest neighbor approximation of the classical Heisenberg model: two collinear, a ferromagnetic (FM) and a row-wise antiferromagnetic (RW-AFM) solutions can be obtained, and two non-collinear solutions, the Néel-state and a SSDW with $\mathbf{q}$-vectors along the line $\overline{\Gamma} - \overline{\mathrm{M}}$ of the Brillouin zone (right). The FM, RW-AFM and Néel-state correspond to SSDWs with $\mathbf{q}$-vectors on the high-symmetry points $\overline{\Gamma}$, $\overline{\mathrm{M}}$ and $\overline{\mathrm{K}}$, respectively.

to the lattice) and the relative angle ϑ between the magnetic moment and the rotation axis. Upon translation by a lattice vector $\mathbf{R}$, the magnetic moment of an atom rotates by an angle $\varphi = \mathbf{q} \cdot \mathbf{R}$. Assuming a rotation around the z-axis (in absence of spin-orbit coupling this is not a loss of generality), the magnetic moment of an atom ν having the basis vector $\boldsymbol{\tau}^\nu$ in the unit cell n (with the origin at the lattice vector $\mathbf{R}_n$) points in the direction

$$\hat{\mathbf{e}}_{n\nu} = \begin{pmatrix} \cos\left(\mathbf{q} \cdot (\mathbf{R}_n + \boldsymbol{\tau}^\nu) + \xi^\nu\right) \sin\vartheta^\nu \\ \sin\left(\mathbf{q} \cdot (\mathbf{R}_n + \boldsymbol{\tau}^\nu) + \xi^\nu\right) \sin\vartheta^\nu \\ \cos\vartheta^\nu \end{pmatrix} . \tag{32}$$

For more than one magnetic atom in the unit-cell, in addition to its basis vector $\boldsymbol{\tau}_\nu$, an additional atom-dependent phase, ξ^ν, appears in the above equation. Nevertheless, the magnetic moments of all atoms rotate around the same axis.

SSDWs are sometimes also called frozen magnons, since a spin-spiral looks like a "snap shot" of a single magnon at a fixed time. Spin-spiral calculations can therefore be used to simulate the effect of temperature on a magnetic system in the adiabatic approximation, in particular at very low temperatures, when magnons with long wavelength dominate (cf. Section 3.3). But also at $T = 0$ many compounds and even elements show SSDW ground states. Some examples are shown in Figure 7.

A very elegant treatment of spin-spirals by first-principle calculations is possible if the generalized Bloch theorem[17,18] is applied. However, this theorem can only be proved, when spin-orbit coupling is neglected. For this reason the spin-rotation axis will always be considered as parallel to the z-axis of the spin coordinate-frame. Thus, only the m_x and m_y components are rotated, while m_z does not change. Following Sandratskii[18], we can define a generalized translation, $\mathcal{T}_n$, that combines a lattice translation, $\mathbf{R}_n$, and a spin rotation $\mathbf{U}$ that commutes with the Hamiltonian H. Applying such a generalized translation to $H\Phi$

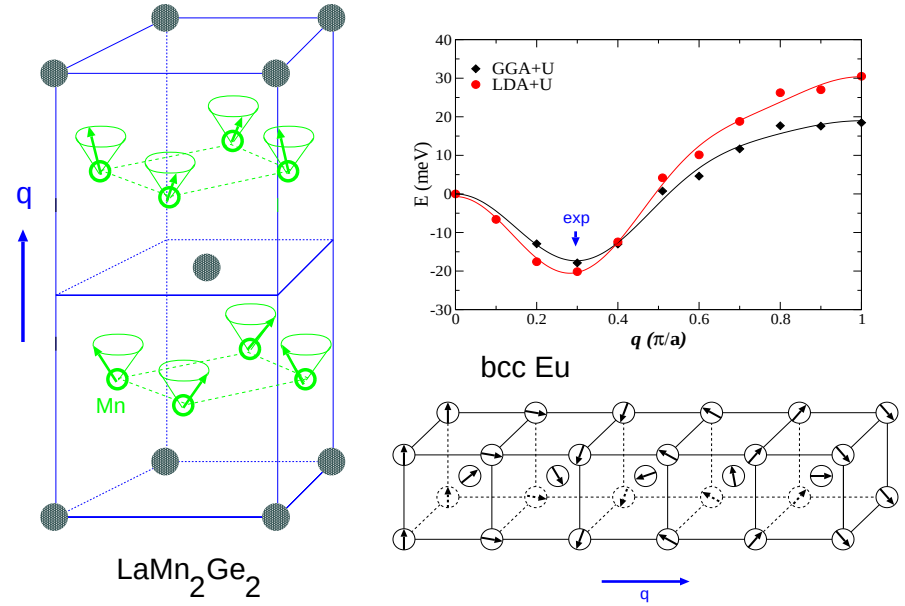

Figure 7. Examples of SSDW ground-states: in $LaMn_2Ge_2$ the spins on the Mn sublattice can be described by a conical spin-spiral with $58°$ semicone-angle and a $\mathbf{q}$-vector of $(0, 0, 0.71)$ in units of $2\pi/c$ (left). Bulk bcc europium has a flat spiral in $[001]$ direction as ground state (right, bottom), the length of the $\mathbf{q}$-vector is correctly reproduced in DFT calculations (right, top).

yields

$$\begin{aligned}\mathcal{T}_n H(\mathbf{r})\Phi(\mathbf{r}) &= \mathbf{U}(-\mathbf{q}\mathbf{R}_n)H(\mathbf{r}+\mathbf{R}_n)\mathbf{U}^\dagger(-\mathbf{q}\mathbf{R}_n)\mathbf{U}(-\mathbf{q}\mathbf{R}_n)\Phi(\mathbf{r}+\mathbf{R}_n)\\ &= H(\mathbf{r})\mathbf{U}(-\mathbf{q}\mathbf{R}_n)\Phi(\mathbf{r}+\mathbf{R}_n)\end{aligned} \tag{33}$$

where $\mathbf{U}(\mathbf{q}\mathbf{R}_n)$ is the spin $1/2$ rotation matrix

$$\mathbf{U}(\mathbf{q}\mathbf{R}_n) = \begin{pmatrix} e^{-i\varphi/2} & 0 \\ 0 & e^{i\varphi/2} \end{pmatrix}, \quad \varphi = \mathbf{q}\cdot\mathbf{R}_n. \tag{34}$$

In analogy with the proof of Bloch's theorem[19] it follows that the eigenstates can be chosen such that

$$\mathcal{T}_n\Phi(\mathbf{k},\mathbf{r}) = \mathbf{U}(-\mathbf{q}\mathbf{R}_n)\Phi(\mathbf{k},\mathbf{r}+\mathbf{R}_n) = e^{i\mathbf{k}\cdot\mathbf{R}_n}\Phi(\mathbf{k},\mathbf{r}). \tag{35}$$

Since these eigenstates are labeled with the same Bloch vector $\mathbf{k}$ as the eigenstates of the translation operator without the spin rotation, the lattice periodic part of these states follows the chemical lattice, $\mathbf{R}_n$, i.e. we can calculate the spin spiral state in the chemical unit cell.

Without the application of the generalized Bloch theorem the investigation of such magnetic structures requires very large unit cells. Since the spin-spiral is the exact solution of the classical Heisenberg model at T$=0$, it is believed that they cover a large and important part of the phase space of possible spin states. Thus among all possible magnetic states, spin-spirals are the next relevant class of spin states besides the high-symmetry magnetic states, i.e. the ferromagnetic, antiferromagnetic, or ferrimagnetic configurations.

3.3 Critical Temperatures, T_{C}, T_{N}

Let us now see, how temperature will influence the magnetic order in a ferromagnetic solid. Staying within the Heisenberg model, we will assume that the magnitude of the magnetic moments at the atoms will – in first approximation – not be changed, and discuss just their mutual orientation. At $T = 0$ the spin at a selected atom will be fixed in parallel direction to the spins at all other atoms by an effective field that will be proportional to $S\sum_n J_{0n} = SJ_0$. At a finite temperature T, this field, acting on the spin at site 0 is reduced due to the thermal fluctuation on the sites n. The thermal average of the projection of the spin at site n on the spin at site 0 is denoted as $\langle S(\mathbf{R}_n)\rangle$. In the "mean field approximation" (MFA), it is assumed that the effective field at finite temperatures that acts on spin 0 is:

$$B_{\mathrm{eff}} = \sum_n J_{0n}\langle S(\mathbf{R}_n)\rangle \tag{36}$$

In this model it is possible to calculate the temperature-dependence of the average magnetization of the solid and, specifically, the temperature where the average magnetization vanishes, the critical temperature. For a ferromagnet this temperature is called Curie temperature and in the MFA it is given by

$$T_{\mathrm{C}} = \frac{2S(S+1)}{3k_{\mathrm{B}}} J_0 \tag{37}$$

It has to be mentioned, that in most cases the MFA severely overestimates T_{C} (by about 20 to 50%, depending on the lattice). Nevertheless, it gives a simple estimate of the ordering temperature in systems, where the approximations of the Heisenberg model are reasonable. On the other hand some properties, like the – material independent – critical exponents, are in any case not reliably reproduced by the MFA.

On a more sophisticated level, the "random phase approximation" (RPA) can give quite reliable results. In contrast to the MFA, where the thermal averaging was done over the sites n that determine B_{eff}, here the Hamiltonian is first transformed into reciprocal space (Eq. (30)), and then the averaging is done over one of the Fourier components:

$$H = -N\sum_{\mathbf{q}} J(\mathbf{q})\mathbf{S}(\mathbf{q})\cdot\langle\mathbf{S}(-\mathbf{q})\rangle \tag{38}$$

If the term $S(S+1)$ is included in the exchange coupling constants (as it is usually done, when the J's are determined from first-principles calculations), then the Curie temperature in the MFA and RPA can be expressed as

$$k_{\mathrm{B}}T_{\mathrm{C}}^{\mathrm{MFA}} = \frac{2}{3}J_0 \qquad k_{\mathrm{B}}T_{\mathrm{C}}^{\mathrm{RPA}} = \frac{2}{3}\left(\sum_{\mathbf{q}}\frac{1}{J(\mathbf{q})}\right)^{-1} \tag{39}$$

From these expressions it is obvious, that calculating T_{C} in the RPA involves not more information that what is needed on a mean-field level, if the exchange coupling constants are calculated in reciprocal space by using the generalized Bloch theorem.

Also for antiferromagnets (or, generally spin-spiral states characterized by a vector $\mathbf{Q}$) expressions for the ordering temperature, the Néel temperature T_{N}, can be derived. In the MFA with $S(S+1)$ again included in J, this is given simply by

$$k_{\mathrm{B}}T_{\mathrm{N}}^{\mathrm{MFA}} = \frac{2}{3}J(\mathbf{Q}) \tag{40}$$

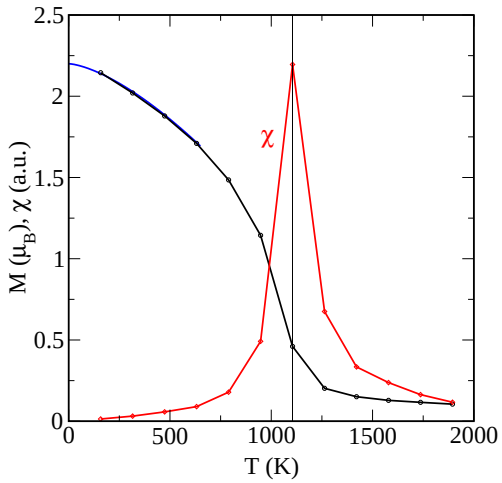

Figure 8. Magnetization, (M), and susceptibility (χ, in arbitrary units) of bulk Fe obtained by MC simulations with several hundred exchange coupling constants taken from *ab initio* calculations[22]. The $T = 0$ behavior of the magnetization is extrapolated by Bloch's law (blue curve). The finite magnetization at $T_{\mathrm{C}} = 1105$K is an artefact of the finite MC simulation super-cell (in this case $10 \times 10 \times 10$ bcc unit cells).

while a slightly more involved expression can be derived in the random phase approximation[20]. Comparison of these results with experimental values gave reasonable results, e.g. for bcc europium Néel temperatures of 147 K and 110 K were obtained in MFA and RPA, respectively[20]. These values have to be compared to the experimental T_{N} of 90.5 ± 0.5 K.

Although there exist several more methods to calculate critical temperatures from DFT results, we will outline here just one further possibility, which seems to be rather flexible and appropriate for many systems with different magnetic ground states: the Monte Carlo technique (MC) allows to study finite-temperature magnetic properties by implementation of a Heisenberg Hamiltonian (Eq. (25), possible with extensions like biquadratic terms or an uniaxial anisotropy (see below)), into a Metropolis algorithm[21]. Unit cells of different size are then studied so that finite-size effects can be eliminated. In these unit cells the evolution of the magnetic property in question (in our case the average magnetization) as a function of temperature can then be monitored (cf. Figure 8).

	T_{C} (K)				
	MFA	MFA2	RPA	MC	exp.
Fe (bcc)	1414	550, 1190	950	1060	1044 – 1045
Co (fcc)	1645	1120, 1350	1311	1080	1388 – 1390
Ni (fcc)	397	320, 820	350	510	624 – 631
Gd (hcp)	334				293

Table 2. Calculated and experimental Curie temperature T_{C} for some ferromagnetic materials. MFA and RPA data for Fe, Co and Ni taken from Padja et al.[23], MFA2 results and experimental values as quoted by Shallcross and coworkers[5], while the MC results were obtained by Rosengaard and Johansson[24]. Data for Gd can be found in the papers of Kurz et al.[6] and Turek and coworkers[25].

Results of *ab initio* calculations of the Curie temperature of Fe, Co and Ni are presented in Table 2. From this table one can easily see that, compared to RPA, the MFA typically overestimates T_{C} by 25–50%. For Fe and Co RPA gives quite good estimates of the Curie temperature, while for Ni T_{C} is underestimated in both approximations. MC simulations work better for Ni and Fe, but give a too low T_{C} for Co. While we quoted here results for "simple" metals, it is nowadays possible to investigate in the same manner the temperature dependent properties of complex multicomponent systems, e.g. half-metallic Heusler alloys[26] or dilute magnetic semiconductors[27].

At low but finite temperatures, collective spin-wave excitations or magnons are excited in the ferromagnetic crystal. These magnons can again be characterized by their wavevector $\mathbf{q}$. In the long wavelength limit, i.e. around $\mathbf{q} = 0$ the spin-wave dispersion behaves almost quadratically and can be described as Dq^2. The spin stiffness, D, characterizes the magnetic properties of a ferromagnet at low temperatures and can also be calculated from the exchange coupling constants:

$$D = \frac{2}{3M} \sum_n J_{0n} R_{0n}^2. \tag{41}$$

Here, M is the magnetic moment of the ferromagnetic state. Some results of *ab initio* calculations are given in Table 3. Again, for Fe and Co agreement with experimental data

	D (meV Å^2)			
	th.(1)	th.(2)	th.(3)	exp.
Fe (bcc)	247	322, 313	250	280, 314, 330
Co (fcc)	502	480, 520	663	510, 580
Ni (fcc)	739	541, 1796	756	422, 550, 555

Table 3. Calculated and experimental spin-wave stiffness (D) for Fe, Co and Ni. The theoretical data was obtained in different approximations as described by Rosengaard and Johansson[24] [th.(1)], Shallcross and coworkers[5] [th.(2)] and Padja et al.[23] [th.(3)], experimental data was taken as cited in these references.

is reasonable, but for Ni most methods fail to reproduce the experimental spin stiffness.

4 Magnetic Anisotropy

In the discussions above, we often assumed that the direction of the magnetic moment(s) is independent from the orientation of the crystal lattice. In many cases, e.g. in bulk crystals like Fe, Co or Ni, this assumption does not lead to qualitatively wrong results, but there are also systems, where the coupling of the spin to the lattice is essential. For example a monolayer of ferromagnetic material, deposited on a nonmagnetic and weakly interacting substrate, would show no long-range magnetic order without this coupling (cf. Section 4.2). But it is also clear that in this case the classical dipole-dipole interaction will be different for a magnetization that is perpendicular to this monolayer or parallel to the surface. For a ferromagnet with only one atom in the unit cell, the dipole energy is given

by

$$E_d = \frac{\mu_B^2}{2} \sum_{n,n'}{}' \frac{m^2}{(\mathbf{R}_n - \mathbf{R}_{n'})^3} \left(1 - 3\cos^2\theta_{nn'}\right) \tag{42}$$

where $\theta_{nn'}$ is the angle between the direction of the magnetic moment $\mathbf{m}$ and the vector connecting $\mathbf{R}_n$ and $\mathbf{R}_{n'}$. In this way, the magnetization of a thin film is always coupled to the crystallographic directions. The fact, that it is more favorable to magnetize a magnetic material in a certain direction than in another direction is then called magnetic anisotropy.

This dipole-dipole interaction always depends on the shape of the macroscopic sample and the resulting magnetic anisotropy is, therefore, called shape anisotropy[28]. But there are also other interactions which lead to magnetically anisotropic behavior, most importantly the spin-orbit coupling discussed in the next section.

4.1 Spin-Orbit Coupling

An electron, traveling with a velocity $\mathbf{v}$ on a classical trajectory around the nucleus, experiences an electric field $\mathcal{E}$ (from the screened nucleus) as a magnetic field, $\mathbf{B} = \frac{1}{c}\mathcal{E} \times \mathbf{v}$. This field will couple to the magnetic (spin) moment μ of the electron as $-\mu \cdot \mathbf{B}$.[a] If we assume, that in a solid the crystal field forces the electron to move e.g. in a certain crystallographic plane, the electron spin will be aligned in a direction normal to this plane. In such a way, a uniaxial anisotropy can arise regardless of the shape of a crystal.

To treat this quantitatively on a quantum-mechanical basis, it is necessary to start from the Dirac equation. In the Schrödinger equation – even for a magnetic system – there is no term that could differentiate the various magnetization directions. But if we include a certain term from the Pauli equation (a two-component approximation to the Dirac equation[30]) we get

$$\left[\frac{\hbar^2}{2m}\nabla^2 + \underline{v}(\mathbf{r}) - \frac{\mu_B}{2mc}\boldsymbol{\sigma} \cdot (\mathcal{E}(\mathbf{r}) \times \mathbf{p})\right] \Phi_i = \epsilon_i \Phi_i. \tag{43}$$

It is this relativistic correction (factor $\frac{1}{c}$) that leads to the coupling between spin-space ($\boldsymbol{\sigma}$) and lattice ($\mathcal{E}(\mathbf{r})$). If we assume that the electric field is derived from a spherically symmetric potential, $V(r)$, (as occurs in the vicinity of an atomic nucleus) we can transform this term

$$\boldsymbol{\sigma} \cdot (\mathcal{E}(\mathbf{r}) \times \mathbf{p}) = \boldsymbol{\sigma} \cdot (\nabla V(r) \times \mathbf{p}) = \frac{1}{r}\frac{dV(r)}{dr}\boldsymbol{\sigma} \cdot (\mathbf{r} \times \mathbf{p}) = \frac{1}{r}\frac{dV(r)}{dr}(\boldsymbol{\sigma} \cdot \mathbf{L}) = \xi \boldsymbol{\sigma} \cdot \mathbf{L}, \tag{44}$$

where $\mathbf{L}$ is the orbital momentum operator. This term is called the spin-orbit coupling (SOC) term with the spin-orbit coupling constant ξ. Since the radial derivative of the potential in a crystal will be largest in the vicinity of a nucleus, we can expect that the major contribution to the spin-orbit interaction will come from this region. For an atom ν then r is the radial part of the vector $\mathbf{r}_\nu = \mathbf{r} - \boldsymbol{\tau}_\nu$. Furthermore, since for small r_ν the potential will be Coulomb-like ($V(r) = -\frac{Z}{r}$), its derivative $\frac{\partial V}{\partial r_\nu}$ is proportional to the

[a] Although this interaction has the form of a Zeeman term (the interaction of the spin with an external magnetic field), due to kinematical effects this spin-orbit interaction is smaller by a factor of two. The origin of this effect is called Thomas-precession[29].

nuclear number of the atom, Z_ν. We thus expect that ξ will be large for heavy atoms, but small for lighter ones.

The magnetocrystalline anisotropy energy (MAE) will then result from the anisotropy of the spin-orbit interaction, i.e. it is the difference of total energies obtained from Hamiltonians including the spin-orbit coupling term with the magnetization pointing in two different directions. Physically, this difference arises due to the crystal field that forces the orbital motion of the electron into a preferred plane[31]. This energy difference is small (in the order of a few μeV's) for bulk systems with high symmetry, e.g. cubic crystals like Fe or Ni. It is larger for crystals with a unique crystallographic axis, like hexagonal Co. But for lower dimensional systems, thin films or atomic wires, the magnetocrystalline anisotropy will essentially determine the magnetic properties, especially at finite temperatures.

4.2 Critical Temperatures in Low Dimensional Systems

In a bulk system, like Fe, the magnetic order is stabilized by exchange interactions against temperature induced fluctuations. The high Curie-temperature $T_\mathrm{C} = 1045\mathrm{K}$ of Fe suggests already that the involved energy scale is about 100 meV ($k_\mathrm{B} = 8.617 \cdot 10^{-5}$ eV/K), and therefore five orders of magnitude larger that typical anisotropy energies in cubic systems. Although the exchange interaction is strong, it is rather short-ranged and decays exponentially with the distance. For two-dimensional systems, Mermin and Wagner[32] showed that no spontaneous magnetization will occur for finite temperatures if the magnetic order is stabilized by an interaction that decays faster than $(\boldsymbol{\tau}_i - \boldsymbol{\tau}_j)^{-n}$ (where the $\boldsymbol{\tau}$'s are the atomic positions and n is a number).

In nature, strictly two-dimensional systems do not occur. Even if only one monolayer of magnetic atoms is deposited on a weakly interacting substrate (like Ag), there is always some interaction between the magnetic atoms via the polarized substrate atoms. But even if this interaction did not exist, there is still a possibility to stabilize magnetic order in this monolayer – via the magnetic anisotropy stemming either from the dipolar or the spin-orbit interaction. For a two-dimensional Heisenberg ferromagnet, Bander and Mills[33] demonstrated that there is indeed a critical temperature if a uniaxial anisotropy is present in the system. If the anisotropy constant is denoted as K and the transition temperature for the same Heisenberg ferromagnet in three dimensions is T_3D, the transition temperature of the two-dimensional system is given by:

$$T_\mathrm{2D} = T_\mathrm{3D} / \ln\left(\frac{3\pi k_\mathrm{B} T_\mathrm{3D}}{4K}\right). \tag{45}$$

In the above mentioned case of uniaxial anisotropy, the energy difference between the situations where a spin $\mathbf{S}$ is perpendicular or parallel to the film normal, chosen to be $\hat{\mathbf{e}}_z$, is given by anisotropy constant K (note, that the different directions in the film plane are assumed to be equivalent here). The uniaxial anisotropy can then be described as a magnetic field $\mathbf{B} = K\hat{\mathbf{e}}_z$, that acts on the spin $\mathbf{S}$. This field gives rise to a Zeeman-term that can be added to the Heisenberg Hamiltonian:

$$H = -\sum_{nn'} J_{nn'} \mathbf{S}_n \cdot \mathbf{S}_{n'} + g\mu_\mathrm{B} \sum_n \mathbf{S}_n \cdot \mathbf{B}. \tag{46}$$

In model Hamiltonian calculations or Monte-Carlo simulations, this type of Hamiltonian can be used when inclusion of an uniaxial anisotropy term is required.

4.3 The Orbital Moment

In section 4.1 we have seen, that in crystalline systems also an orbital motion of the electron around the nucleus occurs, giving rise to a magnetic moment, the orbital moment. Compared to the situation in a free atom this motion is of course restricted by the crystal field that quenches the orbital moment. But spin-orbit coupling provides a mechanism that counteracts this orbital moment quenching and small moments (typically $0.1 - 0.2\mu_{\mathrm{B}}$) can be found (compare Table 1).

The orbital magnetization can be defined in analogy to Eq. (12), expressed in single-particle wavefunctions ϕ_i:

$$\mathbf{m}(\mathbf{r}) = -\mu_{\mathrm{B}} \sum_i \langle \phi_i | \mathbf{r} \times \mathbf{v} | \phi_i \rangle. \tag{47}$$

where $\mathbf{v}$ is the velocity operator. At a certain atom ν, the orbital moment M_ν^{orb} can then be obtained by an integration similar to Eq. (19):

$$M_\nu^{\mathrm{orb}} = -\mu_{\mathrm{B}} \sum_i \langle \phi_i | \mathbf{r} \times \mathbf{v} | \phi_i \rangle_\nu. \tag{48}$$

While this definition of the orbital moment poses no difficulties in periodic solids, we note here that the evaluation of the total orbital moment of a periodic crystal is more involved[34]. In most cases, however, the atomic orbital moments and also the magnetic anisotropy energies, obtained in density functional theory calculations, are too small as compared to experiment. Practical methods that can overcome this deficiency have been discussed in the literature[35].

References

1. P. Hohenberg and W. Kohn, *Inhomogeneous Electron Gas*, Phys. Rev. **136**, B864 (1964).
2. W. Kohn and L. J. Sham, *Self-Consistent Equations Including Exchange and Correlation Effects*, Phys. Rev. **140**, A1133 (1965).
3. U. von Barth and L. Hedin, *A local exchange-correlation potential for the spin polarized case: I*, J. Phys. C: Solid State Phys. **5**, 1629 (1972).
4. V. L. Moruzzi, J. F. Janak, and A. R. Williams, *Calculated Electronic Properties of Metals*, (Pergamon, New York, 1978).
5. S. Shallcross, A. E. Kissavos, V. Meded, and A. V. Ruban, *An ab initio effective Hamiltonian for magnetism including longitudinal spin fluctuations*, Phys. Rev. B **72**, 104437 (2005).
6. Ph. Kurz, G. Bihlmayer, and S. Blügel, *Magnetism and electronic structure of hcp Gd and the Gd(0001) surface*, J. Phys.: Condens. Matter **14**, 6353 (2002).
7. H. W. White, B. J. Beaudry, P. Burgardt, S. Legvold, and B. N. Harmon, *Magnetic moments of ferromagnetic gadolinium alloys*, AIP Conf. Proc. **29**, 329 (1975).
8. V. P. Antropov, M. I. Katsnelson, M. van Schilfgaarde, and B. N. Harmon, *Ab Initio Spin Dynamics in Magnets*, Phys. Rev. Lett. **75**, 729 (1995).
9. V. P. Antropov, M. I. Katsnelson, B. N. Harmon, M. van Schilfgaarde, and D. Kusnezov, *Spin dynamics in magnets: Equation of motion and finite temperature effects*, Phys. Rev. B **54**, 1019 (1996).

10. G. M. Stocks, B. Újfalussy, X.-D. Wang, Y. Wang, D. M. C. Nicholson, W. A. Shelton, A. Canning, and B. L. Györffy, *Towards a constrained local moment model for first principles spin dynamics*, Phil. Mag. B **78**, 665 (1998).
11. P. H. Dederichs, S. Blügel, R. Zeller, and H. Akai, *Ground States of Constrained Systems: Application to Cerium Impurities*, Phys. Rev. Lett. **53**, 2512 (1984).
12. Ph. Kurz, F. Förster, L. Nordström, G. Bihlmayer, and S. Blügel, *Ab initio treatment of noncollinear magnets with the full-potential linearized augmented plane wave method*, Phys. Rev. B **69**, 024415 (2004).
13. B. Újfalussy, X.-D. Wang, D. M. C. Nicholson, W. A. Shelton, G. M. Stocks, Y. Wang, and B. L. Györffy, *Constrained density functional theory for first principles spin dynamics*, J. Appl. Phys. **85**, 4824 (1999).
14. P. W. Anderson, *Theory of Magnetic Exchange Interactions: Exchange in Insulators and Semiconductors*, Solid State Physics **14**, 99 (1963).
15. Ph. Kurz, G. Bihlmayer, K. Hirai, and S. Blügel, *Three-Dimensional Spin Structure on a Two-Dimensional Lattice: Mn/Cu(111)*, Phys. Rev. Lett. **86**, 1106 (2001).
16. K. Yosida, *Theory of Magnetism* (Spinger, Berlin-Heidelberg, 1996).
17. C. Herring, in *Magnetism*, edited by G. Rado and H. Suhl (Academic, New York, 1966).
18. L. M. Sandratskii, *Energy band structure calculations for crystals with spiral magnetic structure*, Phys. Status Solidi B **136**, 167 (1986).
19. N. Ashcroft and N. Mermin, *Solid State Physics* (Saunders College, Philadelphia, 1976).
20. I. Turek, J. Kudrnovský, M. Diviš, P. Franek, G. Bihlmayer, and S. Blügel, *A first-principle study of electronic structure and exchange interactions in bcc europium*, Phys. Rev. B **68**, 224431 (2003).
21. N. Metropolis, A. W. Rosenbluth, M. N. Rosenbluth, A. H. Teller, and E. Teller, Equation of State Calculations by Fast Computing Machines, J. Chem. Phys. **21**, 1087 (1953).
22. M. Ležaić, Ph. Mavropoulos, and S. Blügel, unpublished result (2005).
23. M. Pajda, J. Kudrnovský, I. Turek, V. Drchal, and P. Bruno, *Ab initio calculations of exchange interactions, spin-wave stiffness constants, and Curie temperatures of Fe, Co, and Ni*, Phys. Rev. B **64**, 174402 (2001).
24. N. M. Rosengaard and Börje Johansson, *Finite-temperature study of itinerant ferromagnetism in Fe, Co, and Ni*, Phys. Rev. B **55**, 14975 (1997).
25. I. Turek, J. Kudrnovský,G. Bihlmayer, and S. Blügel, *Ab initio theory of exchange interactions and the Curie temperature of bulk Gd*, J. Phys.: Condens. Matter **15**, 2771 (2003).
26. E. Şaşıoğlu, L. M. Sandratskii, and P. Bruno, *Above-room-temperature ferromagnetism in half-metallic Heusler compounds NiCrP, NiCrSe, NiCrTe, and NiVAs: A first-principles study* J. Appl. Phys. **98**, 063523 (2005).
27. K. Sato, P. H. Dederichs, and H. Katayama-Yoshida, *Is High T_C Possible in (Ga,Mn)N?: Monte Carlo Simulation vs. Mean Field Approximation* J. Supercond. **18**, 33 (2005).
28. S. Blügel, *Magnetische Anisotriopie und Magnetostriktion (Theorie)* in Magnetische Schichtsysteme, Publications by Research Centre Jülich: Matter and materials, Vol.2 (1999).

29. J. D. Jackson, *Classical electrodynamics*, (Wiley & Sons, 1962).
30. H. A. Bethe and E. E. Salpeter *Quantum Mechanics of One- and Two-Electron Systems* (New York, Plenum 1977).
31. J. Stöhr, *Exploring the microscopic origin of magnetic anisotropies with X-ray magnetic circular dichrosim (XMCD) spectroscopy*, J. Magn. Magn. Mater. **200**, 470 (1999).
32. N. D. Mermin and H. Wagner, *Absence of Ferromagnetism or Antiferromagnetism in One- or Two-Dimensional Isotropic Heisenberg Models*, Phys. Rev. Lett. **17**, 1133 (1966).
33. M. Bander and D. L. Mills, *Ferromagnetism of ultrathin films*, Phys. Rev. B **38**, 12015 (1988).
34. T. Thonhauser, D. Ceresoli, D. Vanderbilt, and R. Resta, *Orbital Magnetization in Periodic Insulators*, Phys. Rev. Lett. **95**, 137205 (2005).
35. I. Yang, S. Y. Savrasov, and G. Kotliar, *Importance of Correlation Effects on Magnetic Anisotropy in Fe and Ni*, Phys. Rev. Lett. **87**, 216405 (2001).